Solid state nanofibers based on self-assemblies

Ikkala, Olli; Ras, Robin H. A.; Houbenov, Nikolay; Ruokolainen, Janne; Paakko, Marjo; Laine, Janne; Leskela, Markku; Berglund, Lars A.; Lindstrom, Tom; ten Brinke, Gerrit

Published in:
Faraday Discussions

DOI:
10.1039/b905204f

Publication date:
2009

Solid state nanofibers based on self-assemblies: from cleaving from self-assemblies to multilevel hierarchical constructs

Olli Ikkala,*[a] Robin H. A. Ras,[a] Nikolay Houbenov,[a] Janne Ruokolainen,[a] Marjo Pääkkö,[a] Janne Laine,[b] Markku Leskelä,[c] Lars A. Berglund,[d] Tom Lindström,[e] Gerrit ten Brinke,[f] Hermis Iatrou,[g] Nikos Hadjichristidis[g] and Charl F. J. Faul[h]

Received 13th March 2009, Accepted 31st March 2009
First published as an Advance Article on the web 6th August 2009
DOI: 10.1039/b905204f

Self-assemblies and their hierarchies are useful to construct soft materials with structures at different length scales and to tune the materials properties for various functions. Here we address routes for solid nanofibers based on different forms of self-assemblies. On the other hand, we discuss rational "bottom-up" routes for multi-level hierarchical self-assembled constructs, with the aim of learning more about design principles for competing interactions and packing frustrations. Here we use the triblock copolypeptide poly(L-lysine)-*b*-poly(γ-benzyl-L-glutamate)-*b*-poly(L-lysine) complexed with 2′-deoxyguanosine 5′-monophosphate. Supramolecular disks (G-quartets) stabilized by metal cations are formed and their columnar assembly leads to a packing frustration with the cylindrical packing of helical poly(γ-benzyl-L-glutamate), which we suggest is important in controlling the lateral dimensions of the nanofibers. We foresee routes for functionalities by selecting different metal cations within the G-quartets. On the other hand, we discuss nanofibers that are cleaved from bulk self-assemblies in a "top-down" manner. After a short introduction based on cleaving nanofibers from diblock copolymeric self-assemblies, we focus on native cellulose nanofibers, as cleaved from plant cell wall fibers, which are expected to have feasible mechanical properties and to be templates for functional nanomaterials. Long nanofibers with 5–20 nm lateral dimensions can be cleaved within an aqueous medium to allow hydrogels and water can be removed to allow highly porous, lightweight, and flexible aerogels. We further describe inorganic/

[a]*Department of Applied Physics, Helsinki University of Technology, FIN-02015 TKK Espoo, Finland. E-mail: Olli.Ikkala@tkk.fi*
[b]*Department of Forest Products Technology, Helsinki University of Technology, FIN-02015 TKK Espoo, Finland*
[c]*Department of Chemistry, University of Helsinki, FIN-00014 Helsinki, Finland*
[d]*Department of Fiber and Polymer Technology, Royal Institute of Technology, SE 100 44 Stockholm, Sweden*
[e]*Innventia AB, P.O. Box 5604, SE-114 86 Stockholm, Sweden*
[f]*Zernike Institute for Advanced Materials, University of Groningen, 9747, AGGroningen, The Netherlands*
[g]*Department of Chemistry, University of Athens, Panepistimiopolis Zografou, 157 71 Athens, Greece*
[h]*School of Chemistry, University of Bristol, Bristol, UK BS8 1TS*

organic hybrids as prepared by chemical vapour deposition and atomic layer deposition of the different nanofibers. We foresee functional materials by selecting inorganic coatings. Finally we briefly discuss how the organic template can be removed *e.g.*, by thermal treatments to allow completely inorganic hollow nanofibrillar structures.

Introduction

There exists extensive research towards self-assembled synthetic, biological, and bioinspired soft materials to explore concepts for structural control, increasing complexity, and to achieve various functionalities relevant in applications.[1–7] Self-assemblies can be achieved based on competing repulsive and attractive interactions, where the latter ones can be permanent covalent or weaker physical interactions.[8] Hierarchical structure formation takes place if the different constituent mechanisms act simultaneously at different length scales.[9,10] Nature provides a wealth of examples on self-assemblies allowing tailored materials properties, for example, based on proteins, tough and strong inorganic–organic hybrid structures, plant cell wall cellulosic structures, and multilevel inorganic/organic hierarchical fibrillar constructs.[5,11,12] The last two examples are particularly inspiring for the present paper, in our efforts to investigate different aspects of self-assemblies for rational solid nanofiber construction.

We will first discuss examples of "top-down" methods to cleave solid nanofibers from bulk host self-assemblies, which act as templates for their formation. An extensively used method to prepare nanofibers especially for bioapplications is provided by electrospinning, where even smaller fibers become cleaved due to splaying.[13,14] However, towards the rational use of self-assemblies to construct nanofibers, conceptually perhaps the simplest model material is provided by diblock copolymers[15,16] with hexagonally self-assembled cylindrical cores which can be cleaved by selective solvent processes after shear alignment.[17–19] Such fibers can be post-modified by various ways[20] and we will describe inorganic modification using atomic layer deposition[21] which is a self-limiting sequential chemical vapour deposition concept.[22–24] This allows high precision both in the organic and inorganic parts of the hybrids. On the other, plant cell wall cellulose can be a feasible starting material as it contains within its hierarchical structure mechanically strong native cellulose nanofibers with lateral dimensions of down to a few nm.[12] This in combination with its sustainability has spurred interest for different forms of cellulose in nanoscience and functional materials.[12,25–39] We discuss the cleavage of the native nanofibers (also denoted as microfibrils) to form hydrogels[40] and aerogels,[41] and as an example of their post-functionalization we discuss chemical vapour deposition with TiO_2. In more general terms, widely different functional materials are expected based on different post-modifications.

On the other hand, solid nanofibers can be constructed directly based on self-assemblies "in a bottom-up manner". Nanofiber or nanoribbon formation in aqueous, biological, and solvent environments have received extensive interest, for example by self-assembling helix-coil block copolypeptides, oligopeptide-containing amphiphiles, and even amyloids.[42–47] On the other hand, two-level self-assembled hierarchies and related functional properties have been demonstrated based on supramolecular combinations of block copolymers and surfactants, which allow combinations of structures on the 10–100 nm length scale of block copolymers with length scale structures an order of magnitude smaller than the latter ones.[4,7,9,10] Here we aim to generalize towards higher level hierarchical self-assemblies and structural control by combining several competing motifs, such as competition between disc-like and rod-like mesogens, polypeptides with α-helical, β-sheet and random conformations, additionally involving metal cation binding.[48] This is performed in the context of nanofibers.

Experimental

Sample preparation

Polymeric nanofibers were prepared based on polystyrene-*block*-poly(4-vinylpyridine) (PS-*b*-P4VP) diblock copolymer ($M_{n\mathrm{PS}} = 21.4$ kg mol^{-1}, $M_{n\mathrm{P4VP}} = 20.7$ kg mol^{-1}, $M_w/M_n = 1.13$, Polymer Source, Inc.), pentadecylphenol (PDP) or dodecylphenol (Aldrich), and poly(2,6-dimethyl-1,4- phenylene oxide) (PPE, $M_w = 25.7$ kg mol^{-1}, $M_w/M_n = 1.37$) as described in detail in ref. 17 and 18. The large amplitude shear alignment is made using a dynamic rheometer as also discussed in ref. 17 and 18.

The poly(L-lysine hydrochloride)-*b*-poly(γ-benzyl-d7-L-glutamate)-*b*-poly(L-lysine hydrochloride) (PLL-*b*-PBLG-*b*-PLL) triblock copolypeptide was synthesized from the corresponding precursor poly(ε-*tert*-butyloxycarbonyl-L-lysine)-*b*-poly(γ-benzyl-d7-L-glutamate)-*b*-poly(ε-*tert*-butyloxycarbonyl-L-lysine) by selective deprotection of the ε-amine group of ε-*tert*-butyloxycarbonyl-L-lysine. The precursor was synthesized by sequential ring opening polymerization of γ-benzyl-d7-L-glutamate *N*-carboxy anhydride and ε-*tert*-butyloxycarbonyl-L-lysine *N*-carboxy anhydride with the difunctional initiator 1,6-diaminohexane using high vacuum techniques.[49] The block lengths of PLL-*b*-PBLG-*b*-PLL are $M_{n\mathrm{PBLG}} = 31.0$ kg mol^{-1} and $M_{n\mathrm{PLL}}/2 = 29.9$ kg mol^{-1}, respectively, and the polydispersity index = 1.16.[50] 2′-Deoxyguanosine 5′-monophosphate (dGMP, sodium salt, Sigma–Aldrich) and PLL-*b*-PBLG-*b*-PLL in the HCl form were used to prepare complexes from 3mM KCl aq. solutions at pH 5.2 in a 1:1 (*vs* lysine residue) molar ratio. The concentration of the complex was 90 mM. The complexes precipitated immediately and were centrifuged in cold ethanol, rinsed three times with isopropyl alcohol/H_2O (30/70) mixture and three times with H_2O and dried at ambient conditions.

Native cellulose nanofibers were prepared from bleached sulfite softwood pulp (Domsjö ECO Bright; Domsjö Fabriker AB) consisting of 40% pine and 60% spruce with high hemicellulose content (13.8%) and low lignin content (1%). The fibrillation of the aqueous pulp was achieved by mechanical shearing, enzymatic hydrolysis by monocomponent endoglucanase (Novozym 476, Novozym A/S) followed by washing, mechanical shearing and high-pressure homogenization (Microfluidizer M-110EH, Microfluidics Corp.),[35] which leads to a hydrogel.[40] To prepare the aerogel, the aqueous gel was placed on a mould which was quickly plunged in liquid propane. Thereafter, the frozen sample in the mould was transferred into a vacuum oven and the sample was kept frozen during the drying by a massive cryogenically cooled copper plate underneath. The drying was finished when the pressure in the oven remained stable at *ca.* 10^{-2} mbar.

X-Ray scattering

The small angle X-ray measurements (SAXS) were performed using a Microstar microfocus X-ray source with a rotating anode (CuKα radiation, $\lambda = 1.54$Å) and Montel Optics. The magnitude of the scattering vector is given by $q = (4\pi/\lambda)\sin\theta$, where 2θ is the scattering angle. Wide angle X-ray (WAXS) measurements were performed at the HASYLAB at DESY (Hamburg), Beamline A2.

Chemical vapour deposition and atomic layer deposition

Atomic Layer Deposition (ALD): The Al_2O_3 films were deposited by ALD at 80 °C using trimethylaluminium and H_2O as reactants. The depositions were performed in a F-120 ALD reactor (ASM Microchemistry Ltd., Finland) under a pressure of 10 mbar with N_2 as the carrier and purging gas. One growth cycle consisted of a trimethylaluminium pulse (2 s), a N_2 purge (60 s), a H_2O pulse (0.5 s), and N_2 purge (150 s).

Chemical Vapor Deposition (CVD). TiO_2 films were deposited on dried cellulose nanofibers using an F-120 reactor (Microchemistry Ltd., Finland). The CVD process consisted of pre-heating of the support at 190 °C for 1.5 h; reaction of titanium isopropoxide, $Ti(OC_3H_7)_4$ at 190 °C and 1–5 kPa for 2 h, where the precursor was sublimated at 40 °C and carried with N_2 flow through the chamber; purging with N_2.

Electron microscopy

Bright-field TEM was performed using a Tecnai 12 microscope operating at an accelerating voltage of 120 kV. SEM was performed using Hitachi S-4700 FE-SEM and Leo Gemini DSM 982 microscopes.

Results and discussion

Solid state nanofibers by cleaving from synthetic and biological self-assemblies: "Top-down" nanofiber construction

We will now discuss preparation of solid state nanofibers by cleaving from bulk self-assemblies. Here the main emphasis is cleaving mechanically strong native nanocellulose fibers from macroscopic hierarchically ordered plant cell fibers, but as an introduction we will discuss rational constructs for fiber formation based on synthetic diblock copolymer templates (Fig. 1 Top Part). To this end, diblock copolymers are used which undergo cylindrical self-assembly in bulk. Herein, the cylindrical core is selected to be glassy polystyrene (PS) and it can be reinforced with poly(2,6-dimethyl-1,4-phenylene oxide) (PPE). PPE has a high glass transition temperature (T_g = 216 °C) and due to the molecular level miscibility with PS, its blending increases the glass transition temperature of the core material. Even more importantly, PPE promotes entanglements, and therefore addition of minor fractions of PPE leads to reinforcement, as discussed by van Zoelen *et al.*[18] In order to facilitate simple cleaving, the matrix phase is selected to be poly(4-vinylpyridine) (P4VP) as complexed with alkylphenol: It is well documented based on FTIR that phenols form hydrogen bonds with pyridines, see *e.g.* ref 51. Differential scanning calorimetry shows that alkylphenols, such as dodecylphenol (DDP) or pentadecylphenol (PDP) plasticize P4VP due to the supramolecular spacer-like side chains. If the nonpolar side chain is long enough, such as in PDP, lamellar self-assemblies of $P4VP(PDP)_{1.0}$ are obtained due to the long repulsive side chains.[51] In fact, in PS-*b*-$P4VP(PDP)_{1.0}$ a hierarchical self-assembly at the block copolymer length scale (10–100 nm) and surfactant length scale (*ca.* 3 nm) takes place.[52] For the present PS-*b*-P4VP and the nominally stoichiometric amount of DDP or PDP in comparison to P4VP repeat units, and optionally adding PPE (*e.g.* weight fraction 23% *vs* PS) one obtains cylindrical self-assemblies.[17,18,52] In order to have overall alignment, shear flow processing by either large amplitude dynamic rheometry or, more practically, by an extruder allows high overall alignment.[17,19] Finally, the nanofibers forming the self-assembled cylindrical cores can be cleaved by selective polar solvent treatment using ethanol, thus releasing long individualized nanofibers with a PS core and a P4VP corona, see Fig. 1.[17,18]

These nanofibers can be further functionalized. Here we emphasize that conformal inorganic/inorganic layers, mostly oxide, can be prepared in a well defined way with nanometer precision using ALD. The concept is a specific sequential form of CVD additionally incorporating self-limiting growth. In order to allow combination with the organic block copolymer template, materials and processes requiring low temperature ALD processes have to be selected. As a characteristic example, Al_2O_3 coating is prepared by exposing the nanofibers into a cycle of repeating trimethyl aluminium vapour and humidity, with an inert gas flushing in between. For example, after 200 cycles, Al_2O_3 with a thickness of *ca.* 15 nm is

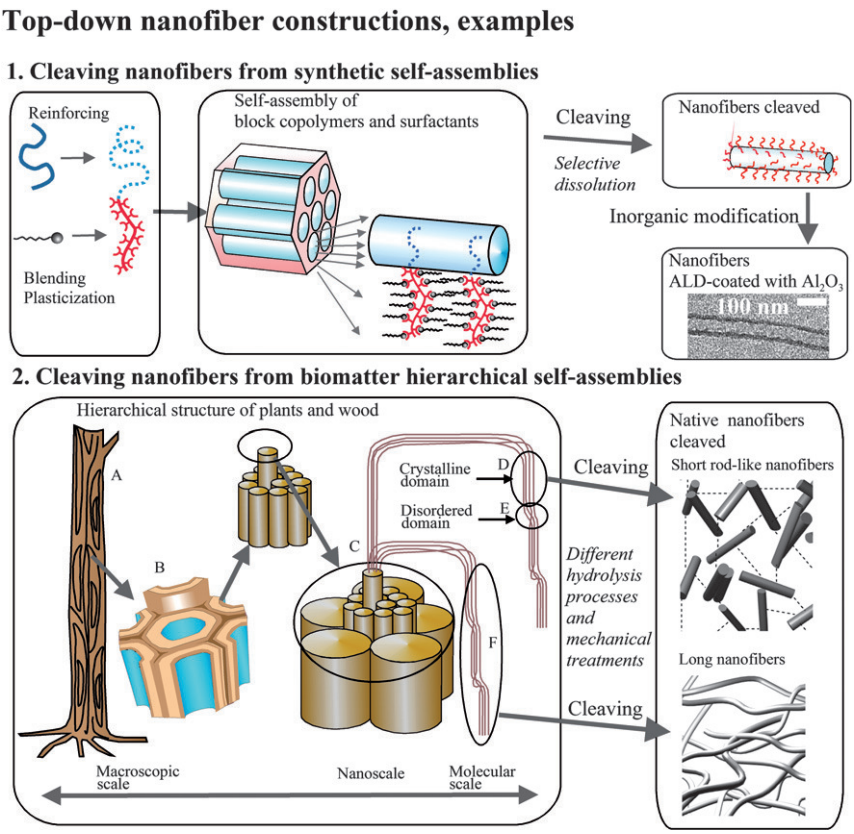

Fig. 1 Examples of cleaving nanofibers from bulk templates. 1: Schematics for a diblock copolymer self-assembled template consisting polystyrene-*b*-poly(4-vinylpyridine) where the polystyrene phase is reinforced with poly(2,6-dimethyl-1,4-phenylene oxide) and poly(4-vinylpyridine) is plasticized using dodecylphenol.[18] Atomic layer deposition allows conformal inorganic coatings where the polymer template can even be removed by heat treatment at the end.[21] 2: Cleaving native cellulose nanofibers from plant cell wall material. Strong acidic hydrolysis leads to rod-like highly crystalline cellulose I nanowhiskers, whereas milder hydrolysis and shearing allows long and entangled native nanofibers. The diameters of the fibers are in the nanometer range. Part of the latter scheme has been adapted from ref. 54.

achieved.[21] Importantly, the TEM micrograph suggests that the inorganic coating is continuous and non-granular (see Fig. 1).

The previous example indicates that combination of polymeric self-assembly and self-limiting inorganic vapour deposition techniques allows well defined inorganic/inorganic matter, where the prerequisite is existence of open surfaces available for the gas phase reactants of ALD, at least during some stage of the process. As ALD allows the construction of various well defined inorganic layers with dielectric and semiconducting properties, the concept paves the way towards functionalized nano-fibers and more generally functionalized inorganic/organic hybrids.

After the above model example, we next describe cleaving high-strength cellulose nanofibers from sustainable plant cell wall templates and their subsequent post-functionalization, of which inorganic CVD is taken as a specific example. We think that such concepts will have substantial importance as sustainable and bioinspired nanomaterials.

Plant cell walls incorporate macroscopic cellulosic fibers (Fig. 1 Bottom Part).[12] They are multicomponent complex materials with a hierarchical internal composition

and structuring at different length scales takes place due to the naturally occurring self-assembly process. Even if the cellulose structure has been in many respects known for cellulose chemists for a long time,[53] the full structural subtleness and possibilities for nanomaterial science has only recently started to be appreciated. Cellulose consists of polysaccharide polymer chains consisting of β-(1→4)-D-glucose repeat units. Due to the biosynthesis, the cellulose chains pack in a specific crystalline I native form in parallel fashion and the chains are mutually interlocked by a substantial amount of hydrogen bonds based on the hydroxyl groups. Therefore, in a lose analogy, the hydrogen bonded structure between the chains in some respects resembles the β-sheets in proteins which act as reinforcements in proteinic materials. The mechanical properties resulting from this native cellulose I crystalline structure are not known in detail as yet, and have been evaluated so far indirectly. The stiffness, as specified by the Young's modulus, is expected to be in the range of 130 GPa.[55] This is high, compared with polymers which typically show 1–4 GPa, aromatic polyamides *ca.* 130 GPa, steel *ca.* 200 GPa, and carbon nanotubes and diamond near 1000 GPa. The strength is difficult to predict, but it is expected to be even up to the range of a few GPa,[39,56] which is comparable with steel *ca.* 0.5–2 GPa and carbon nanotubes, a few tens of GPa. For comparison it is also instructive to compare the predicted values to those of major ampullate silk which has a modulus of 10 GPa and a strength of 1.1 GPa. At the smallest length scale, the cellulose I crystals form nanoscale fibers, that are a few nanometers in the lateral dimension, depending on the cellulose source. They are connected to form long nanoscale fibers *via* disordered domains. Such long nanofibers, in turn, aggregate to form fiber bundles with disordered hemicellulose and lignins. These, in combination with disordered matter are combined at the largest length scale to form the macroscopic cellulose fibers (Fig. 1), which have commonly been used in *e.g.* in papermaking. In conclusion, the macroscopic cellulose fibers have a hierarchically self-assembled structure, which at the lowest level of hierarchy have nanometer fibers with a cellulose I native crystalline structure with expected feasible mechanical properties.

The problem is to prepare distinct cellulose I containing nanofibers. Common procedures to dissolve cellulose or to chemically modify the repeat units generally led to amorphous material or other non-native crystal structures with less than expected optimal mechanical properties. It had already been recognized early on[57,58] that a way could be to cleave the strong nanofibers from the macroscopic fibers by mechanical shearing. In the early days, this typically led to nonuniform materials and the processes were not of extensive practical importance. Recently several interesting methods have been developed based on cleaving the native crystalline cellulose nanofibers by controlled chemical, biochemical, or mechanical treatments that disintegrate the weaker constituents. Acidic hydrolysis leads to extensive hydrolysis of all disordered matter between the nanofibers and also within the disordered domains along the nanofibers, thus leaving only rod-like cellulose nanowhiskers, Fig. 1.[26] They are highly crystalline and have diameters of the order of a few nanometers. Due to their rod-like character and surface charges, they can form liquid crystalline solutions. Here we emphasize that longer, coiled, and entangled nanofibers (Fig. 1) can be obtained if only the interfibrillar disordered matter is disintegrated. Even if purely mechanical treatments were shown to cleave the nanofibers early on, it is only more recently that practical preparations have been developed, *e.g.* based on combination of enzymatic hydrolysis and shearing.[35,40] Here we will discuss efforts to construct nanostructured materials based on such techniques.

As described in the experimental part, following the enzymatic treatment and extensive shearing, the material exists as a dilute mixture in water, typically having a concentration of 0.1–6%wt. Fig. 2A depicts a cryo-TEM micrograph of the aqueous sample, showing a well defined nanofibrillar structure with a lateral dimension of down to *ca.* 5–6 nm, however, thicker occasional bundles are also detected.[40] The micrograph indicates long and entangled nanofibers. This manifests as gelation

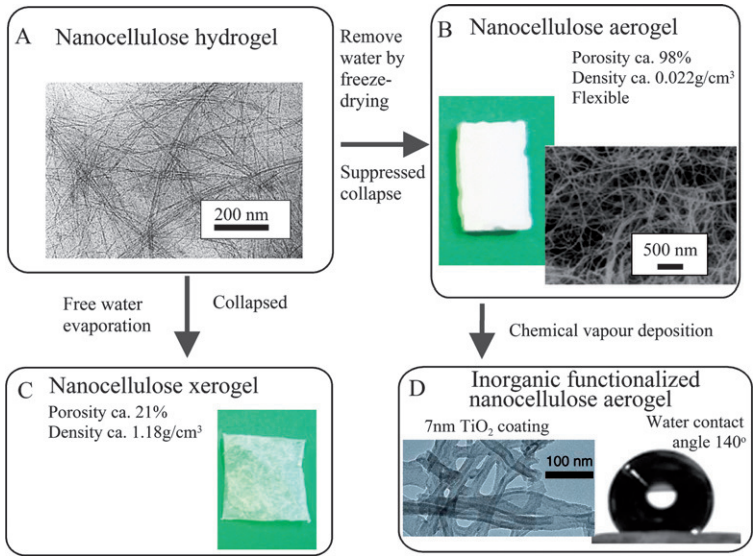

Fig. 2 Native cellulose nanofibers containing cellulose I crystal structure as cleaved from macroscopic cellulose fibers by a combination of enzymatic treatment and shearing. (A) Cryo-TEM of a (aqueous) hydrogel at a concentration of 2%wt, showing mostly 5–6 nm native cellulose nanofibers.[40] (B) Freeze drying to remove water allows lightweight aerogels.[41] Some aggregation of the nanofibers takes place during the water removal. (C) Free evaporation of water from hydrogels leads to a major collapse of the network structure. The samples even start showing some translucence. (D) The aerogels can be modified based on CVD. TEM illustrates TiO_2 coating which leads to a high contact angle by the combined effect of the surface topography and the coating.

in aqueous medium even by visual inspection. In dynamic rheology the storage and loss moduli are essentially independent of frequency for the whole investigated range of concentration from 0.125–6.5%wt and the loss modulus is more than an order of magnitude smaller than the storage modulus. The feasible mechanical properties of the nanofibers manifest themselves as a high value of the storage modulus of 2 MPa for the concentration of 2%wt. This is to be compared with a typical modulus of a rubber. In summary, the long and entangled cellulose nanofibers form a strong aqueous gel.[40]

Here we address the exploitation and functionalization of such nanofibers: for that end the water medium from the aqueous hydrogel is first removed. First, if the water of the hydrogel is just removed by evaporation from the liquid state, a compacted material results due to the collapse of the hydrogel network due to the high surface tension of the water surface receding throughout the sample in the process of drying. The resulting density and porosity depend on the exact method of evaporation, but typically it is *ca.* 1.18 g cm^{-3} and the porosity is around 21% as measured using Hg porosimetry and the material can be denoted as a xerogel (Fig. 2C). After such a drying, the xerogel shows some degree of translucence and sheets thereof show a tensile modulus of *ca.* 6 GPa, a tensile strength of *ca.* 75–80 MPa, and a maximum strain of 2.5%. Such material properties start to be comparable with commodity polymers but obviously such a simple evaporation under laboratory conditions does not allow exploitation of the full mechanical potential of a cellulose nanofiber network. In fact, optimization of the materials and processes allows considerable increases in the values, as shown by Berglund *et al.*: the modulus can be increased to *ca.* 13 GPa and the strength to in excess of 200 MPa by nanocellulose fibers with charged surface groups and using solvent exchange techniques.[36] Also, using various types of nanocellulose, highly transparent films have been obtained

by infiltrating acrylate polymers within the nanocellulose followed by compaction by pressing.[37] Note that the diameter of the fiber is much smaller than the wavelength of light. On the other hand, if the water is removed in the frozen state by using freeze drying, the open hydrogel network structure is essentially preserved even in the dried state without a major collapse.[41] For example, if the hydrogel is simply plunged in liquid propane and the water is subsequently removed in a vacuum oven while keeping the sample frozen, highly porous materials with a very small density of 0.022 g cm^{-3} and high porosity of 98% are obtained (Fig. 2B). Such lightweight and highly porous materials are denoted as aerogels. We point out that aerogel-based inorganic materials, such as silica, as prepared by sol–gel methods form an important class of materials that are extensively used in applications.[59] A common problem therein is that they are very brittle, typically capable of only a fraction of % deformation. However, the present nanocellulose aerogels exhibit a very high deformability without breaking. For example 0.5 mm thick sheets can be reversibly bent back and forth and upon compression the maximum strain is more than 70%; such ultimate compressive strains, however, do not lead to fully reversible deformations.

The nanocellulose aerogels consist of a network of native cellulose nanofibers of diameter of *ca.* 30 nm, see Fig. 2B. Therefore some aggregation has taken place in the process of water removal. The nanofibers have a high density of hydroxyl groups on their surfaces due to the β-(1→4)-D-glucose repeat units. TiO_2 is an interesting oxide material to investigate for functionalization, *e.g.* due to its photocatalytic properties, potential to control wettability, and its possibilities for device making. In an effort to functionalize the native cellulose nanofibers using inorganic matter, CVD of TiO_2 was performed. Dried aerogel was coated by CVD at 190 °C using titanium isopropoxide, $Ti(OC_3H_7)_4$. The detailed analysis is presently in progress based on *e.g.* XPS and spectroscopies and they preliminarily point towards TiO_2 layers. TEM shows a well defined layer of *ca.* 7 nm deposited material on the surface of the native cellulose nanofibers (Fig. 2D). The coating manifests in the wetting behaviour, as expected for TiO_2: A pristine aerogel absorbs a water droplet instantly, so that one can even classify the nanocellulose aerogel as superhydrophilic and superabsorbent. On the other hand, the aerogel with deposited inorganic coating leads to a high contact angle of 130–140°. This is quite high, indicating that the nanocellulose aerogel surface has become extremely hydrophobic. Such high contact angles, approaching those of superhydrophobic materials, are manifestations of a combined effect of surface chemical functionalization and an additional nanoscopic and potentially hierarchical surface topography.

We have shown two routes for organic nanofiber cleaving, based on synthetic block copolymeric bulk self-assembled templating as well as biomatter plant cell fiber templating. We showed that these nanofibers, in turn, are useful templates to grow inorganic coatings. In particular, the ALD is useful for allowing self-limiting well controlled conformal growth. Finally, the organic nanofibrillar template can also be removed, thus allowing us to construct purely inorganic nanoscale hollow objects. We expect that such sequential template routes open up new possibilities for *e.g.* inorganic/organic hybrids, highly porous material and materials for semiconductor devices.

Solid state nanofibers by rational hierarchical construction: "Bottom-up nanofiber construction"

Here we address solid state nanofibrillar constructs containing competing supramolecular discotic and helical rod-like mesogenic groups, which open up systematic ways for more general multilevel hierarchical self-assemblies.[48] In the aqueous and organic solvent medium, there exist extensive efforts to construct nanofibers and nanoribbons based on self-assemblies: One example is provided by diblock copolypeptides with rod-like α-helical blocks and coil-like blocks. Therein, the

lateral dimension of the fibers is controlled by the packing frustration. The α-helical chains have a strong tendency to pack with a small lateral dimension whereas the coiled blocks take more lateral space, depending on the stretching and related entropy.[46] Another approach consists of amphiphiles with oligopeptidic blocks and alkyl blocks, also leading to fiber formation.[42] Rod–coil self-assemblies allow ribbon formation in organic solvents,[43] and nanofibers of rod–coil block copolymers containing conjugated blocks have been investigated *e.g.* for electroactive materials on substrates.[60]

Previously, concepts have been developed for two level self-assemblies by supramolecular combination of block copolymers and surfactants, all based on flexible chains, where the side chains are bonded using *e.g.* hydrogen bonding or ionic bonding.[4,7,52,61] The self-assembly is based on the "chemical" contrast between the three types of constituents. The side-chains can also be rod-like mesogenic, thus incorporating conformation contrast between the constituents to drive towards self-assembling hierarchies.[8] For generalization, we have started to investigate higher level hierarchies by making use of the packing frustration of disks, rods, and coils, in combination with the polypeptide conformational control.[48]

Fig. 3 shows one form which uses packing frustration between rods and disks to allow nanofiber formation. The block copolypeptide (Fig. 3A) consisting of a α-helical poly(γ-benzyl-L-glutamate) (PBLG)[62] central block and two poly(L-lysine) (PLL) hydrochloride endblocks, with molecular weights of 29.9–31.0–29.9 kg mol^{-1}. It has been synthesized using high vacuum techniques using 1,6-diaminohexane initiator as described in the experimental part. Due to the difunctional initiator, the central PBLG block, in fact, consists of two PBLG blocks with a short flexible hexyl spacer in between, see Fig. 3A. For shorthand notation, the block polypeptide is denoted as PLL-*b*-PBLG-*b*-PLL as the overall effect of the short spacer on the central block conformation is expected to be minor, as typically the PBLG helices can have "kinks" anyway within the α-helical conformation.[63] The poly(L-lysine hydrochloride) endblocks are ionically complexed with 2′-deoxyguanosine 5′-monophosphates (dGMP) (Fig. 3B) in aqueous solution containing 3 mM KCl, whereupon segregation takes place after their combination. After centrifuging, rinsing and drying (see experimental part), fibrillation in the solid state was observed using TEM (see Fig. 3G, to be

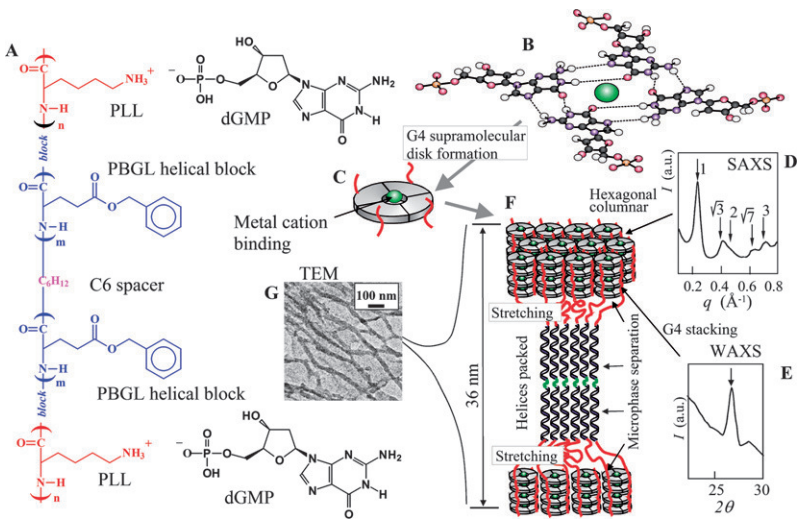

Fig. 3 Hierarchically self-assembled constructs for nanofiber formation,[48] based on competing supramolecular discotic motifs (G-quartets) and helical rod-like motifs (PBLG), block copolypeptide PLL-*b*-PBLG-*b*-PLL microphase separation and metal ion binding.

discussed in more detail later) and also investigated using SAXS and FTIR. For shorthand notation, the resulting ionically complexed adduct is denoted as PLL(dGMP)-*b*-PBLG-*b*-PLL(dGMP).

The structural hierarchy will next be followed step-by-step from the smallest structures up to the largest ones. First, existence of ionic complexation between the phosphoric acid head groups of dGMP and basic lysines of PLL (Fig. 3A) is suggested in FTIR showing distinct absorption peaks at 1059 cm^{-1} due to asymmetric stretching and at 970 cm^{-1} due to the symmetric stretch vibration characteristic for phosphates.[48,64] Elemental analysis shows that in the complex the degree of complexation is 85% *vs* the number of lysine groups. Later we suggest a possible reason for the less than nominally complete complexation, as there has to be an uncomplexed interface region between the block copolypeptide domains, see Fig. 3F later. In general, it is well known that four guanosines tend to form supramolecular discs, denoted as G-quartets or G4, based on 8 hydrogen bonds incorporating so-called Hoogsteen pairings (Fig. 3B and 3C).[65] Such supramolecular discs have a diameter of *ca.* 2.5 nm. Direct spectroscopic evidence is not straightforward to achieve in the present complicated material. However, indirectly the G-quartet formation is unambiguously shown by SAXS (see Fig. 3D), which indicates characteristic reflections at $q_1^* = 0.24$ $Å^{-1}$, $\sqrt{3}q_1^*$, $2q_1^*$, $\sqrt{7}q_1$, and $3q_1^*$, which can be assigned to hexagonal cylindrical packing with a cylinder-to-cylinder distance of *ca.* 3.0 nm. That the cylinder diameter is slightly larger than the diameter of the G-quartets, can be explained due to the PLL complexed with the dGMP within the intercolumnar regions (Fig. 3F). One aspect has to be emphasized: added metal salts are needed to stabilize complexes. In the simplest form, the salt selected is KCl, later we suggest that other salts can also be used to allow functionalities. For PLL(dGMP)-*b*-PBLG-*b*-PLL(dGMP) as prepared in the presence of KCl, WAXS shows a relatively narrow peak at *ca.* 27° (Fig. 3E), which is typical for π-stacking of dimensions 0.33 nm. This indicates that the supramolecular G4 disks stack to form columns (Fig. 3F), as promoted by the cation–dipole interaction between the K^+ cations within the G-quartets. Based on the FTIR evidence on the PLL/dGMP ionic interaction, these columnar assemblies are located in the domains also containing the PLL blocks.

On the other hand, FTIR shows that there are α-helices (1650 cm^{-1} and 1544 cm^{-1}), β-sheets (1693 cm^{-1}, 1631 cm^{-1}, and 1529 cm^{-1}), and random coil (1654 cm^{-1} and 1535 cm^{-1}) conformations within the complex.[48] It is most natural to assess the α-helical conformation to the PBLG, as PBLG is a prototypical coil-forming polypeptide.[62,66] The hexagonal packing of the PBLG helices is supported by X-ray scattering: WAXS shows small but clear reflections that could be assigned as $\sqrt{3}q_2^*$, $2q_2^*$, and $\sqrt{7}q_2$, where the main peak $q_2^* = ca.$ 0.45 $Å^{-1}$ is within the SAXS regime and is masked within a composite reflection peak and cannot be resolved separately. This indicates hexagonal order at the periodicity of 1.3 nm that is close to the value expected for PBLG cylinders.[67] Taken these aspects into account, the central PBLG block has a smaller lateral periodicity due to packed rod-like helical chains whereas the end blocks have a larger periodicity due to the supramolecular disk-like entities. This leads to packing frustration between the PLL(dGMP) end blocks and PBLG central block, while the central and end blocks must microphase separate due to their vastly different natures. TEM (Fig. 3G) gives a hint how the self-assembly is achieved: It indicates fiber formation where the maximum lateral dimension is *ca.* 36 nm. This is closely what would be expected for the PLL-*b*-PBLG-*b*-PLL of the present molecular weight and α-helical central blocks. We also point out that in spite of various staining protocols, the internal structure of the fibers could not be resolved. Neither is SAXS useful for structural assessment due to the small number of block copolypeptide layers within the fibers. Therefore, the exact details leading from packing shown in Fig. 3F to the fibers shown in Fig. 3G are not yet fully elucidated. Finally, we recall that the degree of complexation of dGMP was less than nominal based on the elemental analysis (85%). Taking Fig. 3F, this would be completely expected, as part of the PLL chain

should remain uncomplexed to facilitate connection between the discotic and α-helical domains.

In summary, we suggest that the fiber formation is a manifestation of multilevel hierarchical self-assembly. Recently the G4-assemblies have attracted interest as functional units in assemblies beyond biochemistry.[68] We foresee that the metal cations bound in the cores of the G4-disks obviously due to cation–dipole interactions open up a platform for functionalities: Preliminary results indicate that besides K^+, *e.g.* Fe^{3+} and Tb^{3+} can be loaded within the self-assemblies and investigations are in progress to explore the potential functionalities. We think that judicious selection of the metal cation can open up interesting applications, for example in redox controlled fibers.

Conclusion

We have discussed two routes for nanoscopic solid state fibers based on self-assemblies. The first one can be denoted as a "top down concept", where constituent smaller scale nanofibers are cleaved from macroscopic synthetic or biological bulk self-assemblies. The first example deals with shear aligned diblock copolymeric self-assemblies where the cylindrical cores are cleaved to form distinct fibers. There is more emphasis here on native cellulose nanofibers upon cleaving from macroscopic fibers. Such fibers are expected to have extraordinary mechanical properties and they can allow a useful template for functional nanomaterials. The nanofibers can be post-modified for functionalities using several methods. From the many possibilities, we concentrate here on chemical vapour deposition and atomic layer deposition. In particular, the latter is very feasible in connection with the soft matter and block copolymer self-assemblies, atomic layer deposition is a self-limiting controlled synthesis of inorganic matter. We also describe "bottom-up" solid state nanofibers, based on several length scale self-assemblies. We describe how combining several competing motifs in a rational way, higher level hierarchical self-assemblies are obtained for nanofibrillar constructs, for example by competing discotic and rod-like mesogens, various polypeptide conformations, and microphase separations. We expect interesting new developments for functional materials.

Acknowledgements

We thank P. Hiekkataipale, S. Hanski, S. Funari, M. Kemell, J. de Wit, M. Ritala, W. de Zoelen, G.A. Alberda van Ekenstein, E. Polushkin, H. Nijland, M. Ankerfors, H. Kosonen, A. Nykänen, S. Ahola, M. Österberg, P.T. Larsson, R. Silvennoinen, J. Vapaavuori, V. Pore, L. Wågberg, and J. Sainio for discussions and assistance on the various aspects of the present work. We acknowledge funding from Marie Curie Network 'BioPolySurf', Vinnova, Finnish National Agency for Technology and Innovation, Academy of Finland, UPM, and NOKIA Research Center.

References

1 G. M. Whitesides and B. Grzybowski, *Science*, 2002, **295**, 2418–2421.
2 I. W. Hamley, *Angew. Chem., Int. Ed.*, 2003, **42**, 1692–1712.
3 F. J. M. Hoeben, P. Jonkheijm, E. W. Meijer and A. P. H. J. Schenning, *Chem. Rev.*, 2005, **105**, 1491–1546.
4 O. Ikkala and G. ten Brinke, *Chem. Commun.*, 2004, 2131–2137.
5 M. A. Meyers, P.-Y. Chen, A. Y.-M. Lin and Y. Seki, *Prog. Mater. Sci.*, 2008, **53**, 1–206.
6 C. Park, J. Yoon and E. L. Thomas, *Polymer*, 2003, **44**, 6725–6760.
7 G. ten Brinke, J. Ruokolainen and O. Ikkala, *Adv. Polym. Sci.*, 2007, **207**, 113–177.
8 M. Muthukumar, C. K. Ober and E. L. Thomas, *Science*, 1997, **277**, 1225–1232.
9 O. Ikkala and G. ten Brinke, *Science*, 2002, **295**, 2407–2409.
10 J. Ruokolainen, R. Mäkinen, M. Torkkeli, T. Mäkelä, R. Serimaa, G. ten Brinke and O. Ikkala, *Science*, 1998, **280**, 557–560.

11 J. Aizenberg, J. C. Weaver, M. S. Thanawala, V. C. Sundar, D. E. Morse and P. Fratzl, *Science*, 2005, **309**, 275–278.
12 D. Klemm, B. Heublein, H.-P. Fink and A. Bohn, *Angew. Chem., Int. Ed.*, 2005, **44**, 3358–3393.
13 D. H. Reneker and A. L. Yarin, *Polymer*, 2008, **49**, 2387–2425.
14 G. C. Rutledge and S. V. Fridrikh, *Adv. Drug Delivery Rev.*, 2007, **59**, 1384–1391.
15 F. S. Bates and G. H. Fredrickson, *Phys. Today*, 1999, **52**, 32–38.
16 I. W. Hamley, *The Physics of Block Copolymers*, Oxford University Press, Oxford, 1998.
17 G. Alberda van Ekenstein, E. Polushkin, H. Nijland, O. Ikkala and G. ten Brinke, *Macromolecules*, 2003, **36**, 3684–3688.
18 W. van Zoelen, G. Alberda van Ekenstein, E. Polushkin, O. Ikkala and G. ten Brinke, *Soft Matter*, 2005, **1**, 280–283.
19 A. W. Fahmi, H. Bruenig, R. Weidisch and M. Stamm, *Macromol. Mater. Eng.*, 2005, **290**, 136–142.
20 A. W. Fahmi, H.-G. Braun and M. Stamm, *Adv. Mater.*, 2003, **15**, 1201–1204.
21 R. H. A. Ras, M. Kemell, J. de Wit, M. Ritala, G. ten Brinke, M. Leskelä and O. Ikkala, *Adv. Mater.*, 2007, **19**, 102–106.
22 M. Leskela and M. Ritala, *Angew. Chem., Int. Ed.*, 2003, **42**, 5548–5554.
23 R. L. Puurunen, *J. Appl. Phys.*, 2005, **97**, 121301.
24 M. Ritala and M. Leskelä, in *Handbook of Thin Film Materials*, ed. H. S. Nalwa, Academic Press, San Diego, 2002, pp. 103–159.
25 J.-F. Revol, L. Godbout, X. M. Dong, D. G. Gray, H. Chanzy and G. Maret, *Liq. Cryst.*, 1994, **16**, 127–134.
26 K. Fleming, D. G. Gray and S. Matthews, *Chem.–Eur. J.*, 2001, **7**, 1831–1835.
27 A. N. Nakagaito and H. Yano, *Appl. Phys. A: Mater. Sci. Process.*, 2004, **78**, 547–552.
28 M. A. S. A. Samir, F. Alloin and A. Dufresne, *Biomacromolecules*, 2005, **6**, 612–626.
29 T. Saito, S. Kimura, Y. Nishiyama and A. Isogai, *Biomacromolecules*, 2007, **8**, 2485–2491.
30 O. van den Berg, J. R. Capadona and C. Weder, *Biomacromolecules*, 2007, **8**, 1353–1357.
31 J. R. Capadona, O. van den Berg, L. A. Capadona, M. Schroeter, S. J. Rowan, D. J. Tyler and C. Weder, *Nat. Nanotechnol.*, 2007, **2**, 765–768.
32 A. J. Svagan, M. A. S. A. Samir and L. A. Berglund, *Biomacromolecules*, 2007, **8**, 2556–2563.
33 J. R. Capadona, K. Shanmuganathan, D. J. Tyler, S. J. Rowan and C. Weder, *Science*, 2008, **319**, 1370–1374.
34 S. Ahola, M. Österberg and J. Laine, *Cellulose*, 2008, **15**, 303–314.
35 M. Henriksson, G. Henriksson, L. A. Berglund and T. Lindström, *Eur. Polym. J.*, 2007, **43**, 3434–3441.
36 M. Henriksson, L. A. Berglund, P. Isaksson, T. Lindström and T. Nishino, *Biomacromolecules*, 2008, **9**, 1579–1585.
37 M. Nogi and H. Yano, *Adv. Mater.*, 2008, **20**, 1849–1852.
38 L. Wågberg, G. Decher, M. Norgren, T. Lindström, M. Ankerfors and K. Axnäs, *Langmuir*, 2008, **24**, 784–795.
39 M. Nogi, S. Iwamoto, A. N. Nakagaito and H. Yano, *Adv. Mater.*, 2009, **20**, 1–4.
40 M. Pääkkö, M. Ankerfors, H. Kosonen, A. Nykänen, S. Ahola, M. Österberg, J. Ruokolainen, J. Laine, P. T. Larsson, O. Ikkala and T. Lindström, *Biomacromolecules*, 2007, **8**, 1934–1941.
41 M. Pääkkö, J. Vapaavuori, R. Silvennoinen, H. Kosonen, M. Ankerfors, T. Lindström, L. A. Berglund and O. Ikkala, *Soft Matter*, 2008, **4**, 2492–2499.
42 J. D. Hartgerink, E. Beniash and S. I. Stupp, *Proc. Natl. Acad. Sci. U. S. A.*, 2002, **99**, 5133.
43 L. C. Palmer and S. I. Stupp, *Acc. Chem. Res.*, 2008, **41**, 1674–1684.
44 T. J. Deming, *Adv. Drug Delivery Rev.*, 2002, **54**, 1145–1155.
45 A. P. Nowak, J. Sato, V. Breedveld and T. J. Deming, *Supramol. Chem.*, 2006, **18**, 423–427.
46 T. J. Deming, *Prog. Polym. Sci.*, 2007, **32**, 858–875.
47 T. P. Knowles, A. W. Fitzpatrick, S. Meehan, H. R. Mott, M. Vendruscolo, C. M. Dobson and M. E. Welland, *Science*, 2007, **318**, 1900–1903.
48 N. Houbenov, A. Nykänen, H. Iatrou, J. Ruokolainen, N. Hadjichristidis, C. F. J. Faul and O. Ikkala, *Adv. Funct. Mater.*, 2008, **18**, 2041–2047.
49 T. Aliferis, H. Iatrou and N. Hadjichristidis, *Biomacromolecules*, 2004, **5**, 1653–1656.
50 H. Iatrou, H. Frielinghaus, S. Hanski, N. Ferderigos, J. Ruokolainen, O. Ikkala, D. Richter, J. Mays and N. Hadjichristidis, *Biomacromolecules*, 2007, **8**, 2173–2181.
51 J. Ruokolainen, G. ten Brinke, O. Ikkala, M. Torkkeli and R. Serimaa, *Macromolecules*, 1996, **29**, 3409–3415.
52 J. Ruokolainen, M. Saariaho, O. Ikkala, G. ten Brinke, E. L. Thomas, M. Torkkeli and R. Serimaa, *Macromolecules*, 1999, **32**, 1152–1158.
53 A. C. O'Sullivan, *Cellulose*, 1997, **4**, 173–207.

54 T. Zimmerman, E. Pöhler and T. Geiger, *Adv. Eng. Mater.*, 2004, **6**, 754–761.
55 T. Nishino, K. Takano and K. Nakamae, *J. Polym. Sci., Part B: Polym. Phys.*, 1995, **33**, 1647–1651.
56 D. H. Page and F. EL-Hosseny, *J. Pulp Paper Sci.*, 1983, **9**, 99–100.
57 F. W. Herrick, R. L. Casebier, J. K. Hamilton and K. R. Sandberg, *J. Appl. Polym. Sci.: Appl. Polym. Symp.*, 1983, **37**, 797–813.
58 A. F. Turbak, F. W. Snyder and K. R. Sandberg, *J. Appl. Polym. Sci.: Appl. Polym. Symp.*, 1983, **37**, 815–827.
59 A. C. Pierre and G. M. Pajonk, *Chem. Rev.*, 2002, **102**, 4243–4265.
60 P. Leclere, E. Hennebicq, A. Calderone, P. Brocorens, A. C. Grimsdale, K. Müllen, J. L. Bredas and R. Lazzaroni, *Prog. Polym. Sci.*, 2003, **28**, 55–81.
61 S. Hanski, N. Houbenov, J. Ruokolainen, D. Chondronicola, H. Iatrou, N. Hadjichristidis and O. Ikkala, *Biomacromolecules*, 2006, **7**, 3379–3384.
62 See *e.g.* G. Kess and R. S. Porter, in *Mechanical and Thermophysical Properties of Polymer Liquid Crystals*, ed. W. Brostow, Chapman & Hall, London, 1998, pp. 342–406.
63 P. Papadopoulos, G. Floudas, I. Schnell, T. Aliferis, H. Iatrou and N. Hadjichristidis, *Biomacromolecules*, 2005, **6**, 2352–2361.
64 B. Ozer, C. F. J. Faul, B. Smarsly and M. Antonietti, *Soft Matter*, 2006, **2**, 329–336.
65 J. T. Davis, *Angew. Chem., Int. Ed.*, 2004, **43**, 668–698.
66 P. Papadopoulos, G. Floudas, H.-A. Klok, I. Schnell and T. Pakula, *Biomacromolecules*, 2004, **5**, 81–91.
67 E. A. Minich, A. P. Nowak, T. J. Deming and D. J. Pochan, *Polymer*, 2004, **45**, 1951–1957.
68 H. Cohen, T. Sapir, N. Borovok, T. Molotsky, R. Di Felice, A. B. Kotlyar and D. Porath, *Nano Lett.*, 2007, **7**, 981–986.